

UNDERGROUND TEMPERATURE LOGS FOR WELL FIELD MONITORING

Barbero D.¹, Bucci A.¹, Chiozzi P.², De Luca D. A.¹, Forno M. G.¹, Lasagna M.¹, Verdoya M.²

¹ Earth Sciences Department, University of Turin, Italy

² Earth Sciences, Environment and Life Department, University of Genoa, Italy

1. INTRODUCTION

The study of groundwater flow largely benefits of numerical modeling aimed at searching a more sustainable exploitation of water resources based on the knowledge of the lithostratigraphic setting and information on the aquifer geometry and dynamics from well data (e.g. Lasagna et al., 2014). Continuous monitoring of holes often characterizing well field, represents a hardly practicable solution implying high costs. Alternatively, the analysis of borehole temperatures may improve the local hydraulic characterization and supplying estimates of groundwater flow velocity (Pasquale et al., 2014).

The purpose of this study is to evaluate how borehole thermal logs can contribute to the implementation of a local groundwater flow model. As an example, we study the Maggiore Valley area, located in the Piedmont hilly region (NW Italy) (Fig. 1a), whose main well field supplies drinking water to a wide area and the population of about 100.000 people. The increasing demand of water has led to the overexploitation of the Maggiore Valley groundwater resources, over the past decades, causing progressive lowering of piezometric level, spatial reduction of the artesian zone, localized land subsidence and damage to wells. The piezometric head reduced of about 50 m from 1920 to present-day. The new hydrogeological data inferred with the thermal method can give further constraints for the implementation of groundwater numerical modeling.

2. GEOLOGICAL AND HYDROGEOLOGICAL SETTING

The Maggiore Valley is located at the morphological edge between the Asti Reliefs to the east (130-320 m a.s.l.), and the plain of the Poirino Plateau to the west (240 to 325 m a.s.l.) (Fig. 1a). The stratigraphy of both areas consists of a succession of incoherent sediments, related to depositional environments changing with time from marine to deltaic and fluvial (Carraro Ed., 1996; Forno et al., 2015). The Asti Sands crop out, corresponding to parallel-bedded sands of Pliocene age in the Maggiore Valley, in the lower parts of the reliefs (Fig. 1b and 1d). These sediments are usually covered by the Villafranchian succession, made up with alternations of sands and gravels with silts and clays. The Villafranchian succession continues beneath the Poirino Plateau and consists of two superimposed sedimentary complexes with a total thickness of about 100 m, which are separated by a regional unconformity (Forno et al., 2015). All the sediments display significant deformation linked to the presence of deformation zones (Gattiglio et al., 2016).

Above the Villafranchian succession a continuous cover of fluvial deposits, referred to the middle and upper Pleistocene, is found. These deposits are related to ancient trends of the Po and the Tanaro Rivers and constitute a continuous succession in the Poirino Plateau. The fluvial deposits appear as a terraced fluvial succession that develops at different heights at the top of the hill ridges in the Asti Reliefs (Fig. 1d).

Asti Sands and the Villafranchian succession, both hosting multi-layered aquifer systems, are the most significant water reservoirs. These reservoirs are recharged at the western side of the area by a W-E regional groundwater flow. Both aquifers drain towards East, below the Poirino Plateau, and recharged in Po River plain. Conversely, a medium-permeability shallow aquifer is hosted in the terraces fluvial deposits in the Poirino Plateau, above the multi-layered aquifer previously described (Fig. 1d). This aquifer drains westward and it is mainly fed by direct rainfall and rivers at the outlet of the valley. The water table is strongly influenced by the topography, a wide well field occurs close to the town of Cantarana. Forty-one pumping wells are located on a surface of about 3 km² in the Maggiore Valley and a multi-layered aquifer is hosted in the medium-permeability Asti Sands. A recent piezometric survey in the Maggiore Valley well field (see Lasagna et al., 2014) shows that the extraction of wells activity creates a pronounced depression cone with a W to E flow direction because of the intensive groundwater pumping (Fig. 1c). The magnitude of the hydraulic gradient in the deep aquifer ranges from 1% beneath the Poirino Plateau to 10% in the Maggiore Valley well field.

3. BOREHOLE TEMPERATURE AND SEISMOSTRATIGRAPHY

The position of 5 sites where thermal data were collected is showed in Figure 1. They are located in different hydrological contexts, namely the Poirino Plateau (P2) and Asti Reliefs (P1, P3, P8, P10). In more details, P1-P3 are vertical heat exchangers whereas P8 and P10 are inactive water wells used exclusively for groundwater level monitoring. Temperature measurements were performed using a probe equipped with Pt100 resistances with sensitivity of 0.01 °C.

Wells P1 (170 m a.s.l.) and P3 (156 m a.s.l.) cross the sandy marine succession (Asti Sands) for the whole length. Well P2 (258 m a.s.l.), located in Poirino Plateau is entirely drilled within the Villafranchian succession. The water wells P8 and P10 are placed in the Asti Reliefs in the Maggiore Valley well field (175 m a.s.l.) at a distance of 500 meters each other. Even if they do not undergo pumping activity, they are in the proximity of the cone of depression.

The temperature-depth data recorded in the boreholes are showed in Figure 2. The qualitative analysis of thermal logs clearly indicates that P8 and P10 are dominated by advection. The pattern of the temperature distribution in the two wells may be interpreted as related to a horizontal groundwater flow, occurring in the permeable sandy layers. The

linear trend of other thermal profiles (P1-P3) highlights a prevailing conductive regime. The geothermal gradient ranges from 19 (P2) to 35 mK m⁻¹ (P1) and is consistent with the value of 25 mK m⁻¹ inferred from deep oil wells data (Pasquale et al., 2008).

Distortions on the temperature depth profiles of wells P8 and P10 can be also due to lateral changes in underground thermal properties. Unfortunately, no detailed stratigraphic information is available for these wells. Therefore, in order to understand the stratigraphic setting of the subsoil, a passive seismic survey was performed. Microtremor measurements were carried out with a portable digital tomographer, equipped with three velocimeters orthogonal, recording in the 0.1 to 1024 Hz band. The noise was acquired at 128 Hz sampling frequency, amplified, digitized to 24-bit equivalents and recorded for 20 minutes at each of the measurement sites. Data were analyzed with the Micromed Grilla software and fitted according to the 1-D layered soil theory (Castellaro & Mulargia, 2009).

The seismostratigraphic reconstruction obtained by assuming a shear-wave velocity at the top of 200 m s⁻¹ taking into account the sediment compaction according to Ibs-Von Seht and Wohlenberg (1999) (Fig. 3) The results show the presence of a continuous reflector, all along a cross-section running from P8 to P10. The reflector lies at about 20 m from ground level. Beneath this level, the passive seismic surveys point to a rather homogeneous stratigraphy, likely consisting of sandy succession, arguing that the temperature profile distortions are due to advective perturbations.

4. QUANTITATIVE ANALYSIS OF THERMAL DATA

The analytical procedure of thermal profile analysis consists in matching the experimental measurements of temperature with analytical models of advective heat transfer (see for details Verdoya et al., 2008). For a steady-state thermal and groundwater regime, in permeable horizons with homogeneous thermal and hydraulic properties, the variation of temperature T with depth z can be expressed by Eq. (1), where ρ_w and c_w are the density and specific heat, k is the thermal conductivity and v_x and v_z , supposed to be constant, are the horizontal (positive for a cooling flow) and vertical (positive downward) Darcy velocities, respectively.

$$\lambda \left(\frac{\partial^2 T}{\partial x^2} + \frac{\partial^2 T}{\partial z^2} \right) = \rho_w c_w \left(v_x \frac{\partial T}{\partial x} + v_z \frac{\partial T}{\partial z} \right) \quad (1)$$

Assuming $\partial^2 T / \partial z^2 \gg \partial^2 T / \partial x^2$ and a linear horizontal variation temperature gradient Γ_x , Eq. (1) simplifies as

$$\lambda \frac{\partial^2 T}{\partial z^2} = \rho_w c_w v_z \frac{\partial T}{\partial z} + \rho_w c_w v_x \Gamma_x \quad (2)$$

Far from recharge and discharge areas, the vertical component of velocity can be considered negligible. Therefore, by integrating twice the Eq. (2) with boundary conditions $(\partial T / \partial z)_{z=0} = \Gamma_{z_0}$ and $T = T_L$ for $z = L$, one obtains the following solution

$$T = T_L - \frac{L}{2} (\alpha \Gamma_x + 2 \Gamma_{z_0}) + \Gamma_{z_0} z + \frac{\alpha}{2L} \Gamma_x z^2 \quad (3)$$

where $\alpha = \rho_w c_w v_x L / \lambda$, L is the thickness of the aquifer investigated, T_L the temperature at the base of the portion of the aquifer and Γ_{z_0} the vertical thermal gradient at the depth $z = 0$. Eq. (5) considers Γ_x as uniform, while experimental observations show that the horizontal thermal gradient can depend on depth. Therefore, assuming as a first approximation that Γ_x increases linearly with depth, the solution is

$$T = \left[T_L - L \Gamma_{z_0} - \alpha \Gamma_{x_0} \left(\frac{L}{2} + \frac{L^2 D}{6} \right) \right] + \Gamma_{z_0} z + \frac{\alpha}{2L} \Gamma_{x_0} z^2 + \frac{\alpha}{6L} \Gamma_{x_0} D z^3 \quad (4)$$

where Γ_{x_0} is the horizontal thermal gradient at the upper limit of the aquifer and D (m⁻¹) is a coefficient of variation of Γ_x with depth.

Eqs. (3) and (4) (see Tab. 1) are rewritten in a simplified form more suitable for the optimization procedure. The coefficients of each model can be obtained by the least squares method. The coefficients contain information on the thermal and hydraulic features of the sediments crossed by the wells.

Model	Equation	Coefficient	Horizontal velocity v_x
Eq. (3)	$T = a_1 z^2 + b_1 z + c_1$	$a_1 = \rho_w c_w v_x \Gamma_x / 2\lambda$	$2\lambda a_1 / \Gamma_x c_w \rho_w$
Eq. (4)	$T = a_2 z^3 + b_2 z^2 + c_2 z + d_2$	$b_2 = \rho_w c_w v_x \Gamma_x / 2\lambda$	$2\lambda b_2 / \Gamma_x c_w \rho_w$

Table 1 - Equations in a simplified form of vertical temperature distribution in advective regime with horizontal flow.

The thermal logs of wells P8 and P10, dominated by advection, were analyzed to infer the horizontal component of the Darcy velocity. The estimation v_x requires the horizontal thermal gradient Γ_x which in our calculations was assumed to be equal to $4.8 \cdot 10^{-4} \text{ K} \cdot \text{m}^{-1}$ (Pasquale et al., 2010). The value of Γ_x influences the determination of v_x . In particular, a decrease of one order of magnitude of Γ_x causes an equal increase of v_x . The density ρ_w and specific heat of water c_w were respectively assumed to be $1000 \text{ kg} \cdot \text{m}^{-3}$ and $4187 \text{ J} \cdot \text{kg}^{-1} \cdot \text{K}^{-1}$. As no samples of the sediments crossed by the boreholes were available, a thermal conductivity of $1.8 \text{ W} \cdot \text{m}^{-1} \cdot \text{K}^{-1}$ was assumed on the basis of laboratory determinations of sandstone of the Po Basin (Pasquale et al., 2011).

The values of Darcy velocity obtained for P8 and P10 wells by means of the optimization procedure are reported in Tab. 2. The horizontal Darcy velocity obtained for both wells is of the order of $10^{-6} \text{ m} \cdot \text{s}^{-1}$.

Borehole	Model	Coefficient	R ²	$v_x \text{ (m} \cdot \text{s}^{-1}\text{)}$
P8	Eq. (3)	$a_1 = -3.00 \cdot 10^{-4}$	0.969	$-5.37 \cdot 10^{-7}$
	Eq. (4)	$b_2 = -8.00 \cdot 10^{-4}$	0.999	$-1.43 \cdot 10^{-6}$
P10	Eq. (3)	$a_1 = -2.00 \cdot 10^{-4}$	0.965	$-5.38 \cdot 10^{-7}$
	Eq. (4)	$b_2 = -3.00 \cdot 10^{-4}$	0.999	$-5.37 \cdot 10^{-7}$

Table 2 – Darcy velocities calculated by analytical models coefficients (see Tab. 1). R² is the correlation coefficient.

The horizontal velocities found for the other wells sited out of the Maggiore Valley well field - not shown in Tab. 2 - range between 10^{-7} - $10^{-8} \text{ m} \cdot \text{s}^{-1}$.

5. CONCLUDING REMARKS

The analysis of temperature data recorded in boreholes is a valuable tool for the recognition of underground groundwater flow. Furthermore, through the application of analytical solutions, which describe the expected value of temperature at different depths in sediments affected by processes of heat transport by advection, it is possible to obtain quantitative information on the groundwater velocity.

The velocity values found by thermal methods for P8 and P10 wells are comparable with the velocities introduced in the flow model for the Cantarana well filed, deducted by means of hydraulic properties (hydraulic conductivity $K = 5 \cdot 10^{-5} \text{ m} \cdot \text{s}^{-1}$ and hydraulic gradient $i = 0.1$), validating the numerical model.

On the contrary, the low groundwater flow velocities found for the well placed out of the Cantarana well filed suggest the piezometric map elaborated for the area and its hinterland is correct.

All this information may improve the numerical flow model of Maggiore Valley well field, introducing in the hydrogeological models a warm horizontal flux, located in the Asti Sand at depths greater than 60 meters, with flow velocity of about $10^{-6} \text{ m} \cdot \text{s}^{-1}$, as highlighted by thermal logs.

REFERENCES

- Carraro F. (Ed.); 1996: Revisione del Villafranchiano nell'area-tipo di Villafranca d'Asti. Il Quaternario (It. Journ. Quatern. Sc.), 9 (1): 5–119.
- Castellaro S., Mulargia F., 2009: Vs30 estimates using constrained H/V measurements. Bulletin of the Seismological Society of America, Vol. 99, (2A): 761–773.
- Forno M.G., Gattiglio M., Comina C., Barbero D., Bertini A., Doglione A., Irace A., Gianotti F., Martinetto E., Mottura A., Sala B.; 2015: Stratigraphic and tectonic notes on the Villafranca d'Asti succession in type-area and Castelnuovo Don Bosco sector (Asti reliefs, Piedmont). Alpine and Mediterranean Quaternary, 28(1), 5-27
- Gattiglio M., Forno, M.G., Comina, C., Doglione A., Violanti, D. and Barbero, D.; 2015: The involving of the Pliocene-Pleistocene succession in the T. Traversola Deformation Zone (NW Italy). Alpine and Mediterranean Quaternary, 28(1), 59-70.
- Ibs-von Seht M., Wohlenberg J.; 1999: Microtremor measurements used to map thickness of soft sediments. Bull. Seismol. Soc. America, 89, 250-259.
- Lasagna M., Caviglia C., De Luca D.A.; 2014: Simulation modeling for groundwater safety in an overexploitation situation: the Maggiore Valley context (Piedmont, Italy). Bull. Eng. Geol. Environ., 73,341–355.
- Pasquale V., Chiozzi P., Gola G., Verdoya M.; 2008: Depth-time correction of petroleum bottom-hole temperatures in the Po Plain, Italy. Geophysics, 73, 187–196

Pasquale V., Verdoya M., Chiozzi P.; 2010: Evaluation of heat and water flow in porosity permeable horizons. *Boll. Geofis. Teor. Appl.*, 51, 361-371.

Pasquale V., G. Gola, P. Chiozzi., Verdoya M.; 2011: Thermophysical properties of the Po Basin rocks. *Geophy. J. Inter.* 186, 69-81.

Pasquale V., Verdoya M., Chiozzi P.; 2014: *Geothermics, heat flow in the lithosphere*. Springer, Heidelberg, 119 pp.

Verdoya M., Pasquale V., Chiozzi P.; 2008: Inferring hydro-geothermal parameters from advectively perturbed thermal logs. *Inter. J. Earth Sc.*, 97, 333-344.

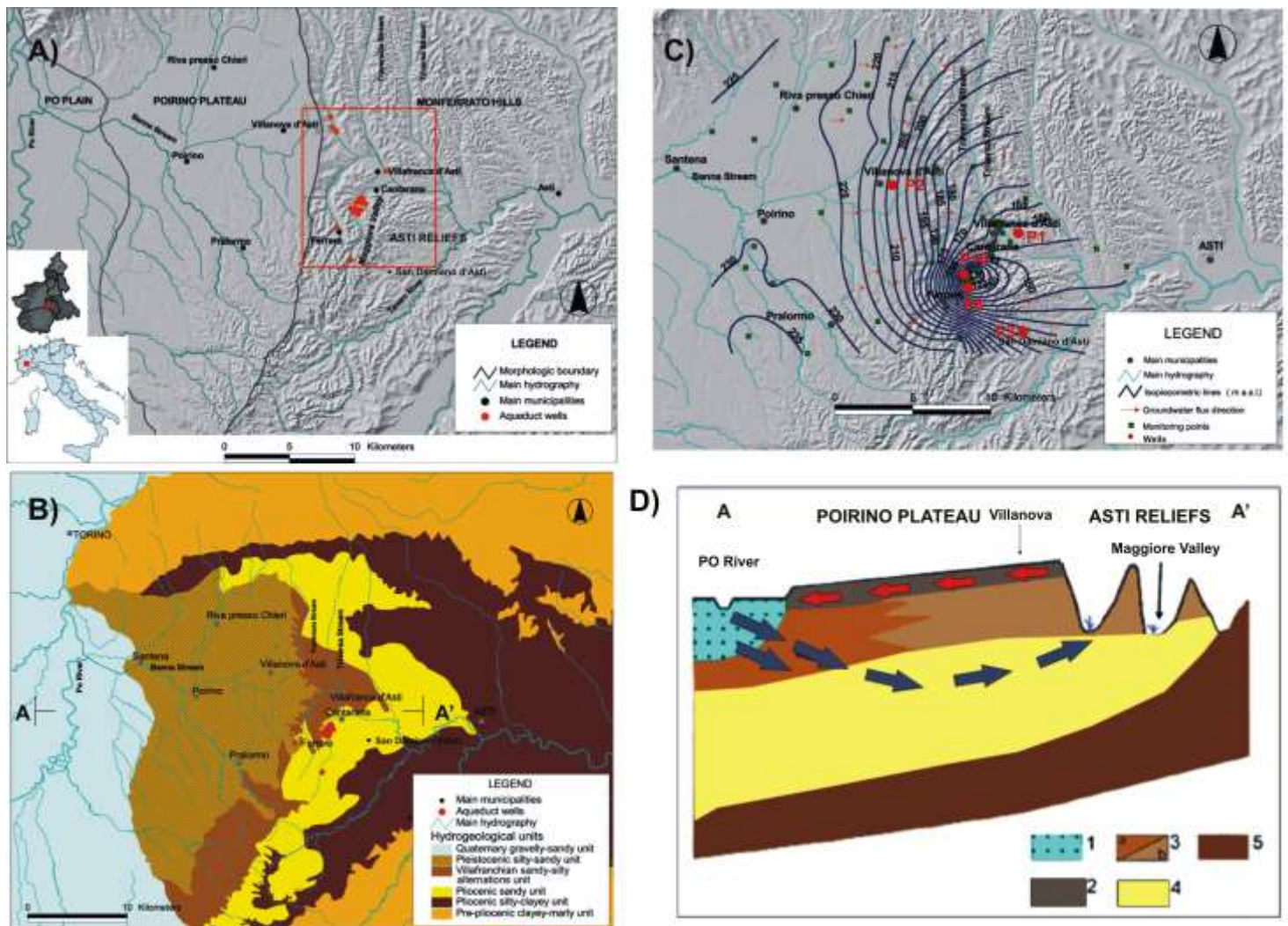


Fig. 1 – Location of well field (A), hydrogeological complexes (B) and piezometric map (C) of the Maggiore Valley. Hydrogeological conceptual model (D): 1 Holocene fluvial deposits; 2 Pleistocene fluvial deposits; 3 Villafranchian succession (Piacenzian – Calabrian) (a: silt and clay; b: gravel and sand); 4 Asti Sands (Zanclean); 5 Lugagnano Clay (Piacenzian). Arrows indicate the groundwater flow direction (from Lasagna et al., 2014).

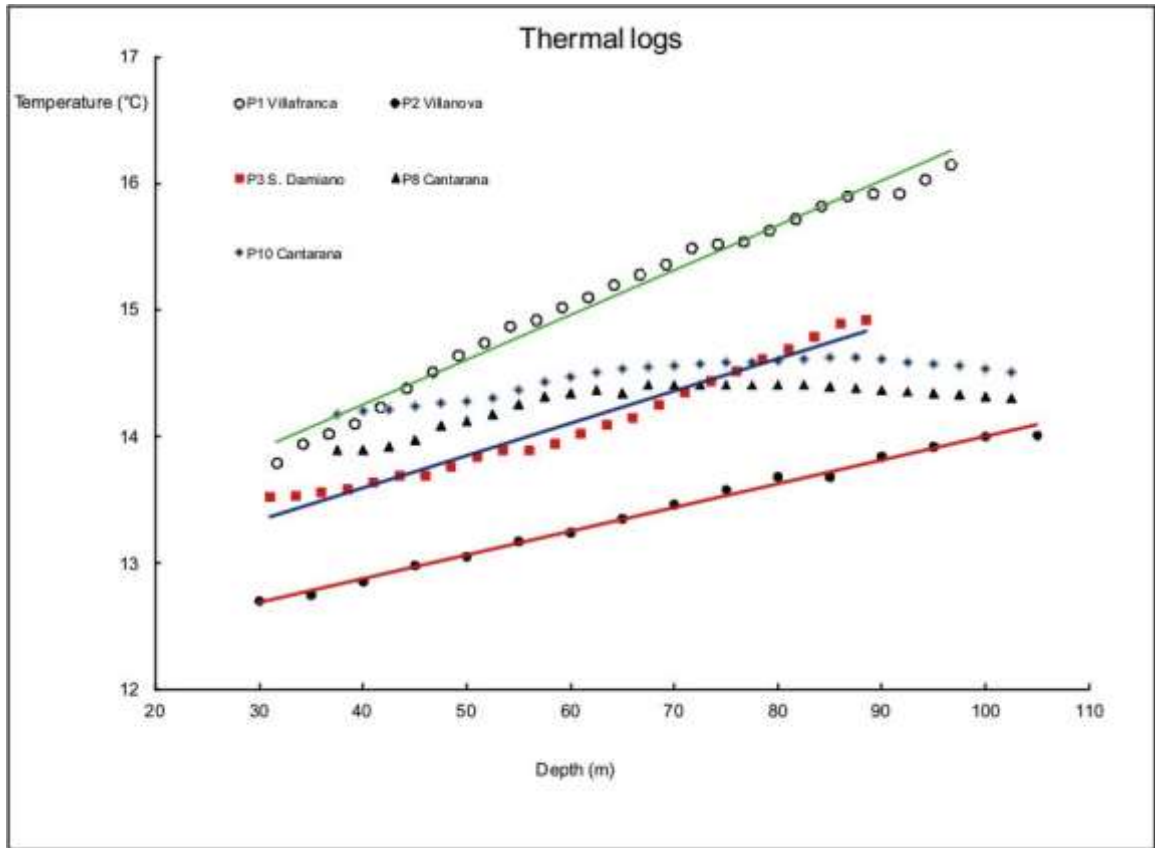


Fig. 2 –Thermal logs recorded in the Maggiore Valley and surroundings (see Fig. 1 for wells location)

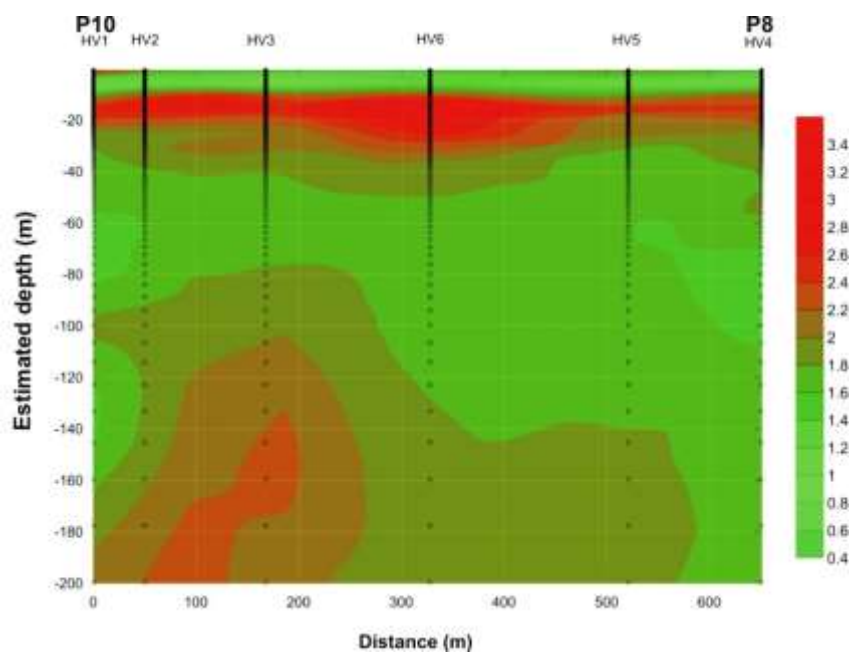


Fig. 3 –Seismo-stratigraphic model: the colors indicate impedance contrasts; HV1-HV6 are measurement sites, P8 and P10 water wells.